PHOENICS Newsletter

CHAM

Contents:

Dear Reader

We are moving forward to a point when we will be able to operate "normally" which, in the case of CHAM, means a return to working, as a team, based physically at our Wimbledon Village headquarters.

We are also moving forward, with the release of PHOENICS-2021 which will include enhanced graphics, new features, updates, and improvements (see the "sneak preview" on page 7 of this Newsletter).

As mentioned in News from CHAM, page 7, we are in the final stages of making PHOENICS available via the Microsoft Azure Cloud.

The first Online User Meeting, for Dutch and German Users, is being arranged by CHAM agent Frank Kanters of Coolplug BV on June 11 2021. For more information contact Frank.Kanters@coolplug.com.

Our Summer Newsletter is in production. Please share PHOENICS, FLAIR, or RhinoCFD, experiences by sending articles (in Microsoft Word) to news@cham.co.uk. We look forward to hearing from you.

All at CHAM continue to work to support Users, and to provide our software, consulting, technical, and other, services. Please do not hesitate to get in touch.

Kind Regards

Colleen Spalding
Managing Director

Spring 2021

Wave forces for multiple objects, by Saliha Nouri, Zouhair Hafsia, Salah Mahmoud Boulaaras, Ali Allahem and Salem Alkhalaf, Qassim University, Saudi Arabia,

Introduction

The new capability of the PHOENICS code to compute the wave forces applied by a multiple object is tested in the case of four cylinders under the effect of solitary waves. The wave force applied on a single cylinder is taken as a reference case. The wave force $\vec{F}$ acting on each cylinder is computed by integrating the water pressure p and the normal component of the viscous stress tensor τ on the wetted surface of the cylinder:

$$\vec{F} = \int_S (-\vec{n}\, p + \vec{n}.\tau)\, dS$$

Where $\vec{n}$ is the normal unit vector pointing into the water. This flow field problem is relevant to offshore oil platforms and coastal bridges composed by multiple cylinders. When the wave run-up and following wave forces exceed expected values, the safety of these structures is compromised. The main tasks of the wave structure interaction (WSI) model are prediction of wave run-up, forces, breaking, and flow separation. Wave diffraction near multiple cylinders depended on the interference flow fields following the gap distance between the cylinders. A full three-dimensional numerical wave tank (NWT) was integrated in the PHOENICS code in order to study solitary wave diffraction with different cylinders arrangements. The solitary wave was generated by an internal source line [1]; cylinder structures are discretized using the cut-cell method; the Volume Of Fluid (VOF) method is adopted to predict the evolution of the water level [2].

Wave diffraction by an oil platform

When a solitary wave passes around a single cylinder, run-up occurs at the front of the cylinder; maximum run-up depends on incident wave energy. The water level then drops at the front causing the water level at the rear of the cylinder to rise by the process of wave diffraction.
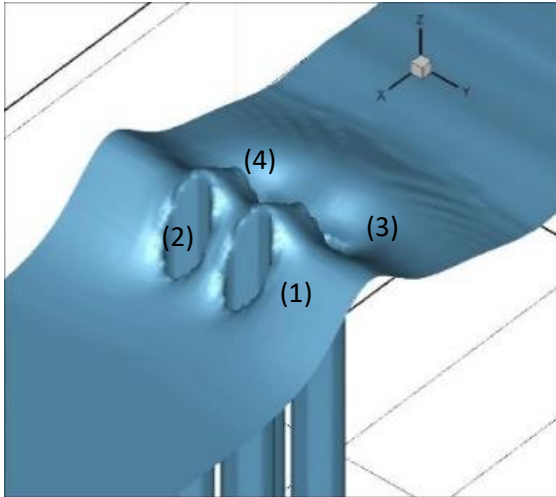
Interaction of the solitary wave with an oil platform composed of four vertical circular cylinders is investigated for a square and diamond arrangement as indicated in Figure 1. The depth-to-cylinder-radius ratio is: $\frac{h}{a} = 1$; distance from the center of the cylinders is $S = 3\, a$. The cut-cell method is used to mesh the circular cylinders in a Cartesian coordinate system.

The perspective view of the free surface elevation is shown in Figure 1 at the instant of the maximum run-up at cylinder 1. The solitary wave crest has been altered by the diffraction process. Impacting the cylinder obstacle, the wave run-up is observed due to the transformation of the incident wave to potential energy. R_{max} depends on the incoming wave and the nature of the obstacle.

For the square arrangement, R_{max} for the first array (cylinders 3 and 4) occurs at the instant t = 2.90s and for second array (cylinders 1 and 2) at t = 3.45s. For the diamond arrangement, the first R_{max} is observed for the most upstream cylinder (4) at t = 2.88s. The maximum run-ups for cylinders 2 and 3 occur at the same instant (t = 3.16 s) and, due to non–linear effect, R_{max} for cylinder 1 is observed at t = 3.48 s. For the diamond arrangement, R_{max}/H for cylinders 4 and 1 located at the centerline approach to that on the isolated cylinder. R_{max}/H for cylinders 2 and 3 is slightly greater than on the isolated cylinder. Due to wave field interference, the maximum run-up on the downstream cylinder is less than that on the upstream cylinder. This interference effect is known as the shielding effect of the upstream cylinder on the downstream one.

Interaction of the solitary wave with an oil platform composed of four vertical circular cylinders is investigated for a square and diamond arrangement as indicated in Figure 1. The depth-to-cylinder-radius ratio is: $\frac{h}{a} = 1$; distance from the center of the cylinders is $S = 3\, a$. The cut-cell method is used to mesh the circular cylinders in a Cartesian coordinate system.
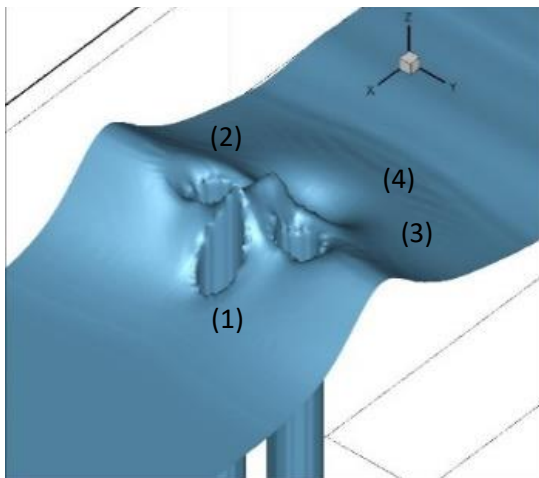
(a)

(b)

Figure 1: A three-dimensional free-surface elevation at the maximum run-up of the cylinder 1 for H/h = 0.25: a) Square arrangement; b) Diamond arrangement.

The time evolution of the wave force in the positive x–direction for each cylinder is presented in Figure 2 for the square and diamond arrangements. Maximum wave force F_{max} on the most downstream array of the cylinders (1 and 2) is slightly greater than on the isolated cylinder.

The increase of F_{max} relative to the isolated cylinder is more pronounced for the first cylinder array (cylinders 3 and 4). The platform and wave interaction leads to F_{max} for the first cylinder array (3 and 4) greater than on the second array (1 and 2). This can be attributed to the shielding effect of the upstream cylinder array. These conclusions are in concordance with the computed run-ups previously discussed.

In the diamond arrangement aligned cylinders 4 and 1 have the same F_{max} which is significantly smaller than the isolated cylinder. The two symmetric cylinders at the centerline of the computational domain have the same F_{max} as the isolated cylinder. The approaching solitary wave for these cylinders seems not to be disturbed by the diffraction process.
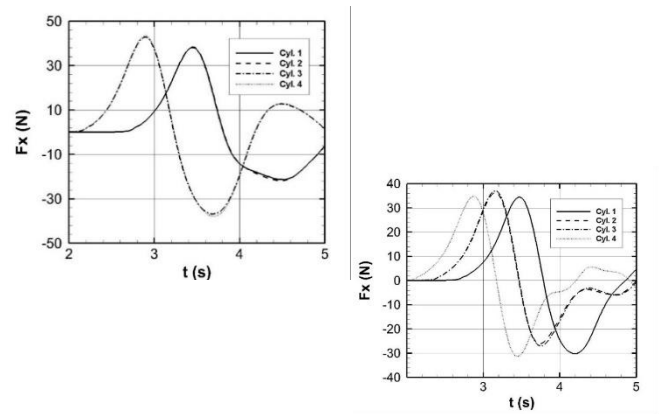

Figure 2: Time evolution of the in-line force on an oil platform for H/h = 0.25; a) square arrangement; b) diamond arrangement.

References:

[1] Hafsia Z., Ben Haj M., Lamloumi H. and Maalel K. Internal inlet for wave generation and absorption treatment. Coastal Engineering 56, pp. 951-959, 2009.

[2] Hafsia Z., Nouri S., Boulaaras S. M., Allahem A., Alkhalaf S. and Vazquez A. M. - Solitary Wave Diffraction with a Single and Two Vertical Circular Cylinders. Mathematical Problems in Engineering Volume 2021, Article ID 6634762, 9 pages.

The investigation of the influence of the distance between convector plates on the heat flux, by Afonina n.g., glazov v.s, MEI.

Setting of the task

The main goal of this investigation is to study the impact of the distance between plates into a convector on temperature and air velocity on the outlet from a heat exchanger. The investigative tool was PHOENICS. The convector-plate parameters are presented in Figure 1. Serial connections of such plates allows the formation of different models of convectors, which are differentiated only by size δ.
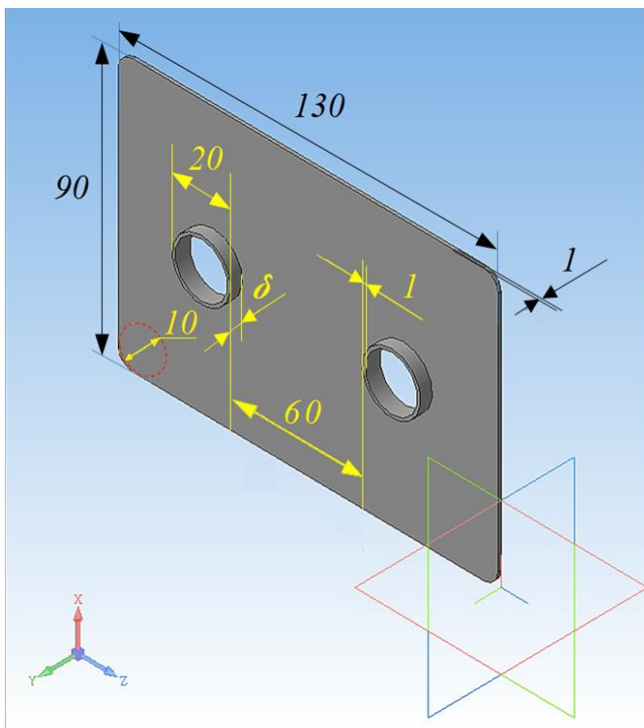

Figure 1 – Parameters of plate in convector (δ = 9, 6, 4 and 1.5 mm)

The temperature of environmental air is set at 20⁰C. The steel cylinders (diameter 20 mm and length 70 mm) are formed where the plates connect and have a temperature of 80⁰C. The heat conduction of plate material is 43 W/(m K). Results of the numerical simulation are processed by MathCad to determine the best choice of the plate step in convector.

Numerical Simulation

The exchange of convector and environmental air heat in the system was investigated using PHOENICS. The main stages of investigation were:

- creation of construction in VR-Editor;
- setting boundary conditions;
- grid creation;
- Result analysis and preparation of data for MathCad.

Results of simulation and its processing in MathCad

X-coordinates of the cell centres
```
1.227E-03  3.477E-03  5.000E-03  6.906E-03  1.000E-02
1.309E-02  1.500E-02  1.691E-02  2.000E-02  2.309E-02
2.500E-02  2.691E-02  3.000E-02  3.309E-02  3.500E-02
3.691E-02  4.000E-02  4.309E-02  4.500E-02  4.691E-02
5.000E-02  5.309E-02  5.500E-02  5.691E-02  6.000E-02
6.309E-02  6.500E-02  6.662E-02  6.887E-02  7.135E-02
7.431E-02  7.786E-02  8.213E-02  8.725E-02  9.339E-02
```

Y-coordinates of the cell centres   2.727E-03

Z-coordinates of the cell centres   3.333E-01

$x_9 :=$

	1	2	3	4	5
1	$1.227 \cdot 10^{-3}$	$3.477 \cdot 10^{-3}$	$5 \cdot 10^{-3}$	$6.906 \cdot 10^{-3}$	0.01
2	0.013	0.015	0.017	0.02	0.023
3	0.025	0.027	0.03	0.033	0.035
4	0.037	0.04	0.043	0.045	0.047
5	0.05	0.053	0.055	0.057	0.06
6	0.063	0.065	0.067	0.069	0.071
7	0.074	0.078	0.082	0.087	0.093

$$X_9 := stack\left[\left(x_9^T\right)^{\langle 1\rangle}, \left(x_9^T\right)^{\langle 2\rangle}, \left(x_9^T\right)^{\langle 3\rangle}, \left(x_9^T\right)^{\langle 4\rangle}, \left(x_9^T\right)^{\langle 5\rangle}, \left(x_9^T\right)^{\langle 6\rangle}, \left(x_9^T\right)^{\langle 7\rangle}\right]$$

$$t1 := \begin{pmatrix} 6.839E+01 \\ 7.181E+01 \\ 7.179E+01 \\ 7.161E+01 \\ 6.685E+01 \end{pmatrix} \quad t2 := \begin{pmatrix} 7.177E+01 \\ 7.189E+01 \\ 7.201E+01 \\ 6.699E+01 \\ 7.192E+01 \end{pmatrix} \quad t3 := \begin{pmatrix} 7.164E+01 \\ 7.145E+01 \\ 6.531E+01 \\ 7.099E+01 \\ 7.083E+01 \end{pmatrix} \quad t4 := \begin{pmatrix} 7.069E+01 \\ 6.366E+01 \\ 7.006E+01 \\ 7.027E+01 \\ 7.048E+01 \end{pmatrix}$$

$$t5 := \begin{pmatrix} 6.359E+01 \\ 6.990E+01 \\ 7.020E+01 \\ 7.048E+01 \\ 6.468E+01 \end{pmatrix} \quad t6 := \begin{pmatrix} 6.950E+01 \\ 6.114E+01 \\ 5.731E+01 \\ 3.902E+01 \\ 2.115E+01 \end{pmatrix} \quad t7 := \begin{pmatrix} 2.000E+01 \\ 2.000E+01 \\ 2.000E+01 \\ 2.000E+01 \\ 2.000E+01 \end{pmatrix} \quad T_9 := stack(t1, t2, t3, t4, t5, t6, t7)$$

Figure 2: MathCad's listing of data processing of file result. Distance between plates in convector is 9 mm
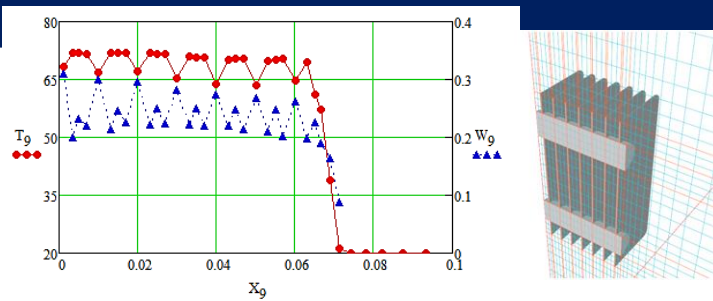
Figure 3: Temperature distribution in the zone near heat exchanger and grid, which was used at simulation.
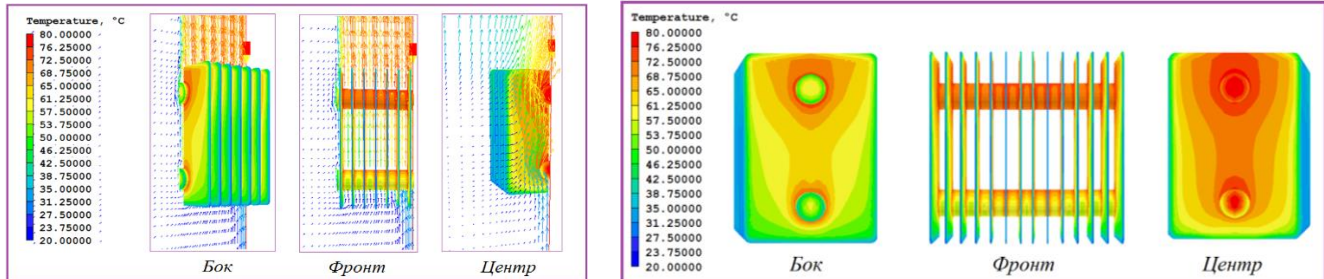

Figure 4: Temperature distribution on the surface of convector and velocity in convector
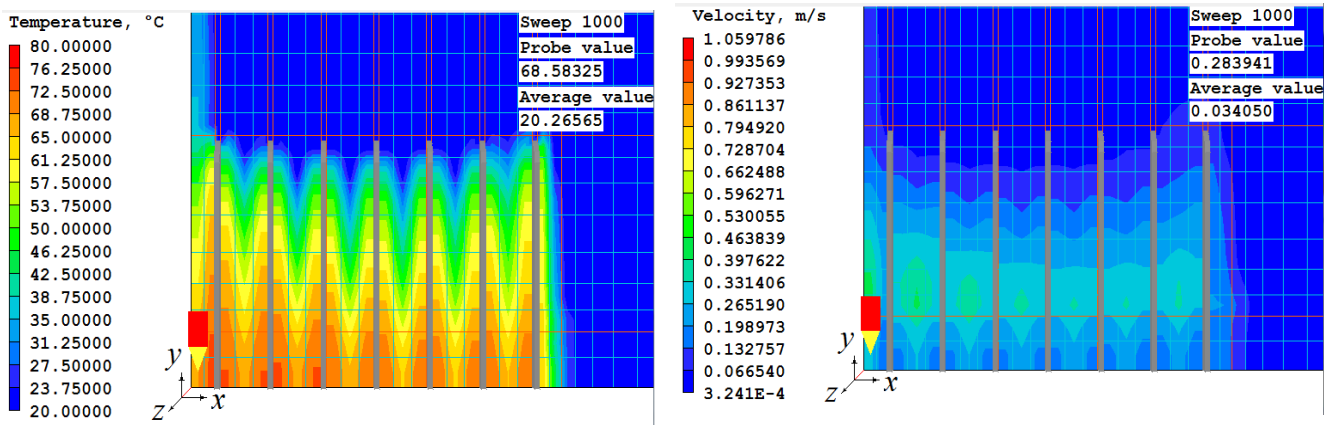

Figure 5: The temperature and velocity distribution on the outlet of convector

Convectors constructed with steps between plates from 1.5 mm to 10 mm were simulated. Table 1 contains sample results.

Table 1: Convector Parameters

Step of plates into convector, mm	Number of plates on length 140 mm	Specific heat flux $q \times 10^{-4}$, W/m²	Volume density of heat source, $Q \times 10^{-6}$, W/m³
2.5	56	0.429	0.914
7	20	1.559	3.317
10	14	1.371	2.916

Conclusion

It was concluded, from the calculated data, that the best variant of heat exchanger was that with a step between plates equal to 7mm as higher values of specific heat flux and volume density of heat source are visible.

An online course entitled "Particle-laden flows: Theory and engineering applications" has been developed in the context of a collaborative research project financed by the T.I.M.E. association (www.timeassociation.org). The project, led by Politecnico di Milano, involved four other partner institutions, namely, Czech Technical University in Prague (Czech Republic), University of Campinas (Brazil), Xi'an Jiaotong University (China), and Xi'an Shiyou University (China).
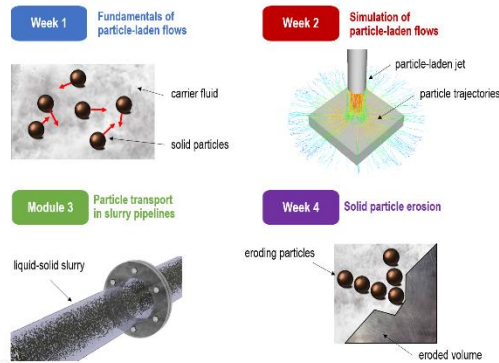

Figure 1. The four "weeks" of the online course

As the title itself says, the course is focused on particle-laden flows, i.e. two-phase flows of a carrier fluid and solid particles, and it develops around the research expertise and interest of the teachers. Particularly, the course consists of 18 video lessons divided into four modules, called "weeks", dedicated to the fundamentals of particle-laden flows, the simulation of particle-laden flows, the particle transport in slurry pipelines, and the solid particle erosion, respectively (Figure 1).

In addition to the theoretical lessons, taught by me and Vaclav Matoušek from Czech Technical University in Prague, several case studies have been kindly provided by the other project partners, as well as by invited contributors. These include both colleagues from academic institutions, such as Federal University of Uberlândia (Brazil), Ecole Polytechnique Fédérale de Lausanne (Switzerland), Pontificia Universidad Católica de Chile, MCI – The Entrepreneurial School (Austria), and two industrial companies, namely, CHAM Ltd and ENI S.p.A (Italy).

Case studies provided by Harry Claydon and Michael Malin from CHAM, entitled "CFD application cases involving particle-laden flows", comprise three PHOENICS application examples relevant to the topic of the course.

These are: the modelling of a gravity dust catcher in a steelmaking plant, the modelling of aerosol deposition in a building using FLAIR, and an investigation of the turbulence modulation in gas-solid two-phase jets. Relevant pictures from the three application examples are shown in Figure 2.
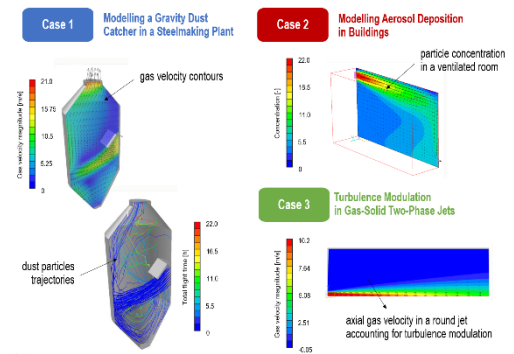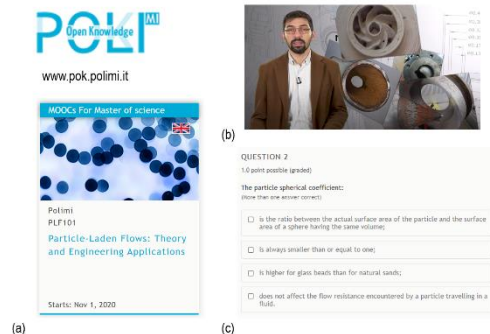

Figure 2. Pictures from the three case studies provided by CHAM

The course is now available, free of charge, on the POK portal of Politecnico di Milano (Figure 3) using the following link:

https://www.pok.polimi.it/courses/course-v1:Polimi+PLF101+2020_M11/about
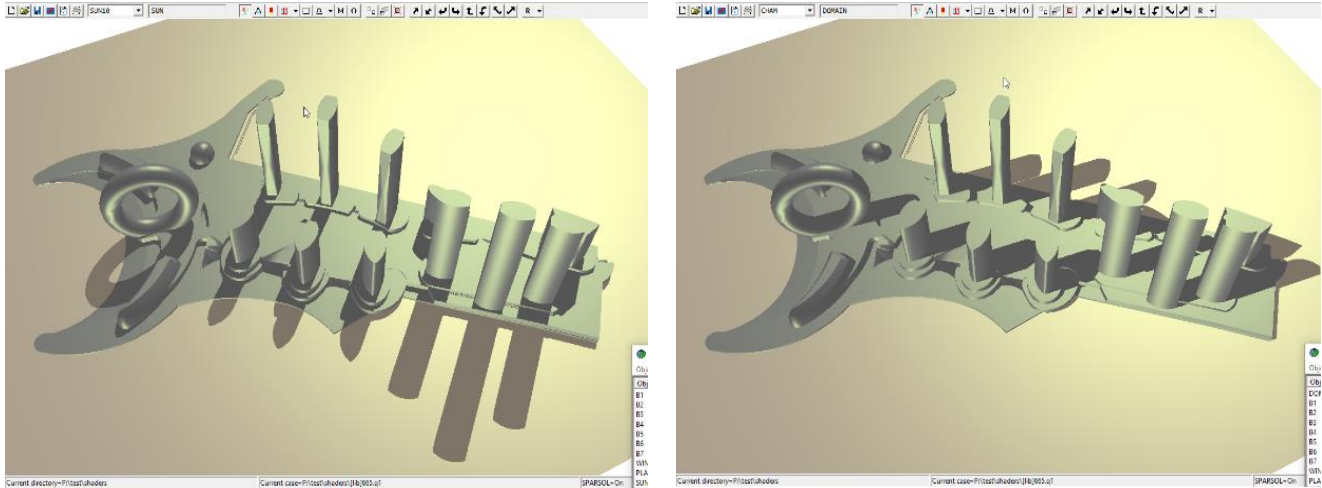
People enrolled in the course can attend the video lessons and access the case studies. After successful completion of 60% of the questions, a certificate of accomplishment can be requested. The first edition of the online course, which started in April 2020 and ended in October 2020, had 216 participants. The second edition is now coming to an end, but the next one will start on 1st March 2021. Currently, Gianandrea Vittorio Messa is cooperating with Torsten Fransson, professor at KTH Stockholm and member of the T.I.M.E association, to make the online course available also on the Learnify platform (www.learnify.se/en/), with the support of the METID office at Politenico di Milano, Qi Yang, and Vaclav Matoušek.

PHOENICS 2021

This is a sneak pre-view of a few items planned for the first release of PHOENICS 2021:

- PHOENICS will be available on the Cloud. Final details are yet to be decided but technical trials are underway.
- A Linux version will be available, using Wine, to allow the VR Editor and VR Viewer to operate exactly as under Windows whilst retaining a native Linux solver.
- Enhanced graphics in the VR editor and VR Viewer using VBO shaders which will include better handling of transparency and will allow display of shadowing and solar shading (without the need to run the Solver). The images show buildings in Dubai at 8 am and 3 pm using the PHOENICS 2021 solar shading model.

- Simplified selection of object shapes, and improved import of CAD.
- Ability to set the domain origin to an arbitrary location, not always at (0,0,0).
- Improved detection and display of double-cut cells for Parsol.

PHOENICS 2020v1.3

Since the release of PHOENICS 2020v1.0 earlier in the year, several minor deficiencies have been reported by users, and have been remedied. Rather than delay until PHOENICS 2021 is ready (hopefully end Q1 2021), it has been decided to release an update to PHOENICS 2020 which addresses issues raised and includes some general improvements.

Improvements

- For Immersol, the link between H1 and T3 in solid cells has been made the same as the existing link between TEM1 and T3, This greatly improves the speed of convergence of linked equations when energy is solved in enthalpy form. This is particularly applicable to cases with combustion.
- The InForm operator {}, used to obtain the value of a variable at a physical (x,y,z) location no longer interpolates between neighbour cells when dealing with the PRPS or OBID variables. For these, it just returns the value in the cell containing the specified coordinate.
- For linked ANGLED-IN objects, it is now possible to specify minimum and maximum exit temperatures. This prevents a cooler reducing exit temperature below temperature of the cooling coils, or a heater increasing exit temperature above the temperature of the heating element. For this release, the limits have to be edited into the Q1 file as SPEDAT commands; in the future this will be extended to all scalars via the VR Editor. The commands needed are: SPEDAT(object_name,TMIN,R,minimum_temperature) and SPEDAT(SET,object_name,TMAX,R,maximum_temperature).

- The InForm Editor used to edit InForm commands into the Q1 has been replaced by PQ1Ed, which is already used to edit Q1 and RESULT files. There is now a common editor used for all file-editing functions from with the VR Editor.
- The TECPLOT interface has been improved to produce the translated output files from parallel runs.

  Binary output from the double-precision solver has been corrected, and a flag has been added to cham.ini to switch between binary and ascii output. The stand-alone TECPLOT translator has been given command-line arguments to specify input and output file names, so it can be used to process many files in batch mode.

Corrections

- Corrections have been made to the Drift Flux Model used in Flair to represent the spread and settling of aerosols. In particular, corrections have been made to the parallel operation of the model. Another correction was to prevent deposition on solid surfaces shared with inlets or outlets, as strictly speaking there is no solid surface there.
- Corrections have been made to the integration of pressure- and friction-force over the surfaces of solid blockages within a ROTOR object.

Special account has to be taken of the movement of the objects, and also when an object passes through the cyclic boundary at X=0 and 2π. In essence, the integration used to be over the original location of the objects without taking account of their movement. The total, pressure and friction torques are now output separately. An error which meant that the torque and moment-about-Z were not equal has been corrected.

- Improvements have been made to the treatment of cyclic boundary conditions in polar coordinates, leading to smoother contours across the X=0 and 2π boundary.
- It has been reported that in some cases the Sparsol detection of complex geometries was not as good as in PHOENICS 2019. This has been addressed, and the detection should be as good as previously.
- It has been found that, very rarely, cells could be marked as 'belonging' to a source object, when in fact they were outside the facets of the object. This could lead to sources appearing in unexpected places. The possibility has been removed.
- In InForm, corrections have been made to the SUM() function in parallel.

Licensed users wishing to update to this version should contact Millie Lyle at: ml@cham.co.uk.

The first Online User Meeting to be held for Dutch and German users being arranged by CHAM agent, Frank Kanters of Coolplug BV on 10th June 2021. More information from Frank.Kanters@coolplug.com. http://www.coolplug.com/

Contact Us:

Should you require any further information regarding our offered products or services please give us a call on +44 (20) 89477651; alternatively you can email us on sales@cham.co.uk.

Visit our website at www.cham.co.uk; we are also on the following social media sites: